JCI insight

RESEARCH ARTICLE

Site-1 protease–derived soluble (pro)renin receptor targets vasopressin receptor 2 to enhance urine concentrating capability

Fei Wang,[1,2] Chuanming Xu,[1,2] Renfei Luo,[1,2] Kexin Peng,[1,2] Nirupama Ramkumar,[1] Shiying Xie,[1,2] Xiaohan Lu,[1,2] Long Zhao,[1] Chang-Jiang Zuo,[1] Donald E. Kohan,[1] and Tianxin Yang[1,2,3]

[1]Department of Internal Medicine, University of Utah and Veterans Affairs Medical Center, Salt Lake City, Utah, USA. [2]Institute of Hypertension, Zhongshan School of Medicine, Sun Yat-sen University, Guangzhou, China. [3]Institute of Hypertension and Renal Disease, The First Affiliated Hospital of Zhengzhou University, Zhengzhou, China.

The antidiuretic hormone vasopressin (AVP), acting through its type 2 receptor (V_2R) in the collecting duct (CD), critically controls urine concentrating capability. Here, we report that site-1 protease–derived (S1P-derived) soluble (pro)renin receptor (sPRR) participates in regulation of fluid homeostasis via targeting V_2R. In cultured inner medullary collecting duct (IMCD) cells, AVP-induced V_2R expression was blunted by a PRR antagonist, PRO20; a PRR-neutralizing antibody; or a S1P inhibitor, PF-429242. In parallel, sPRR release was increased by AVP and reduced by PF-429242. Administration of histidine-tagged sPRR, sPRR-His, stimulated V_2R expression and also reversed the inhibitory effect of PF-429242 on the expression induced by AVP. PF-429242 treatment in C57/BL6 mice impaired urine concentrating capability, which was rescued by sPRR-His. This observation was recapitulated in mice with renal tubule–specific deletion of S1P. During the pharmacological or genetic manipulation of S1P alone or in combination with sPRR-His, the changes in urine concentration were paralleled with renal expression of V_2R and aquaporin-2 (AQP2). Together, these results support that S1P-derived sPRR exerts a key role in determining renal V_2R expression and, thus, urine concentrating capability.

Introduction

The antidiuretic hormone, 8-arginine vasopressin (AVP), plays a key role in determining the urine concentrating capacity, a major function of the mammalian kidney in maintaining fluid homeostasis (1). The action of AVP is mediated by G-protein–coupled receptors called AVP receptors that exist in 3 subtypes: V1, V2, and V3. V2 receptors (V_2R) are the major receptor subtype responsible for the antidiuretic action of AVP, which activates adenylyl cyclase type VI and increases cyclic cAMP levels (2), leading to activation of major ion and water transport proteins in the distal nephron. In the collecting duct (CD), activation of this pathway results in redistribution of aquaporin-2 (AQP2) to the apical membrane of the principal cells, allowing precise control of water excretion (3, 4). Besides the CD, the water-impermeable thick ascending limb (TAL) is another important site of antidiuretic action of AVP. The NKCC2-mediated Na^+ transport in the TAL is a prerequisite for maintaining the longitudinal osmotic gradient and is activated by the AVP-V_2R axis (5, 6).

(Pro)renin receptor (PRR) is a 350–amino acid type 1 transmembrane receptor that binds both prorenin and renin with high affinity in the nanomolar ranges (7–9). Within the kidney, PRR is predominantly expressed in the intercalated cells of the CD. Multiple studies using genetic and pharmacological approaches consistently demonstrate an essential role of renal tubular PRR in regulation of urine concentrating capability (10, 11). In this regard, deletion of PRR from the whole nephron (10, 12) and the CD (13) in mice consistently produces diabetes insipidus (DI), while administration of a PRR decoy inhibitor PRO20 in rats impairs urine concentrating capability (13).

Full-length PRR is subjected to protease-mediated cleavage to produce a 28 kDa of the N-terminal extracellular domain, the soluble PRR (sPRR) and the 8.9 kDa C-terminal intracellular domain called M8.9 (14, 15). We have shown in vitro evidence that sPRR, via β-catenin signaling, stimulates AQP2 expression in cultured CD cells (16). Based on these observations, we proposed a potentially novel paracrine model: sPRR is produced from intercalated cells and secreted to the urine, and it then acts on the neighboring principal

Conflict of interest: The authors have declared that no conflict of interest exists.

Submitted: August 13, 2018
Accepted: November 29, 2018
Published: January 10, 2019

Reference information:
JCI Insight. 2019;4(1):e124174. https://doi.org/10.1172/jci.insight.124174.

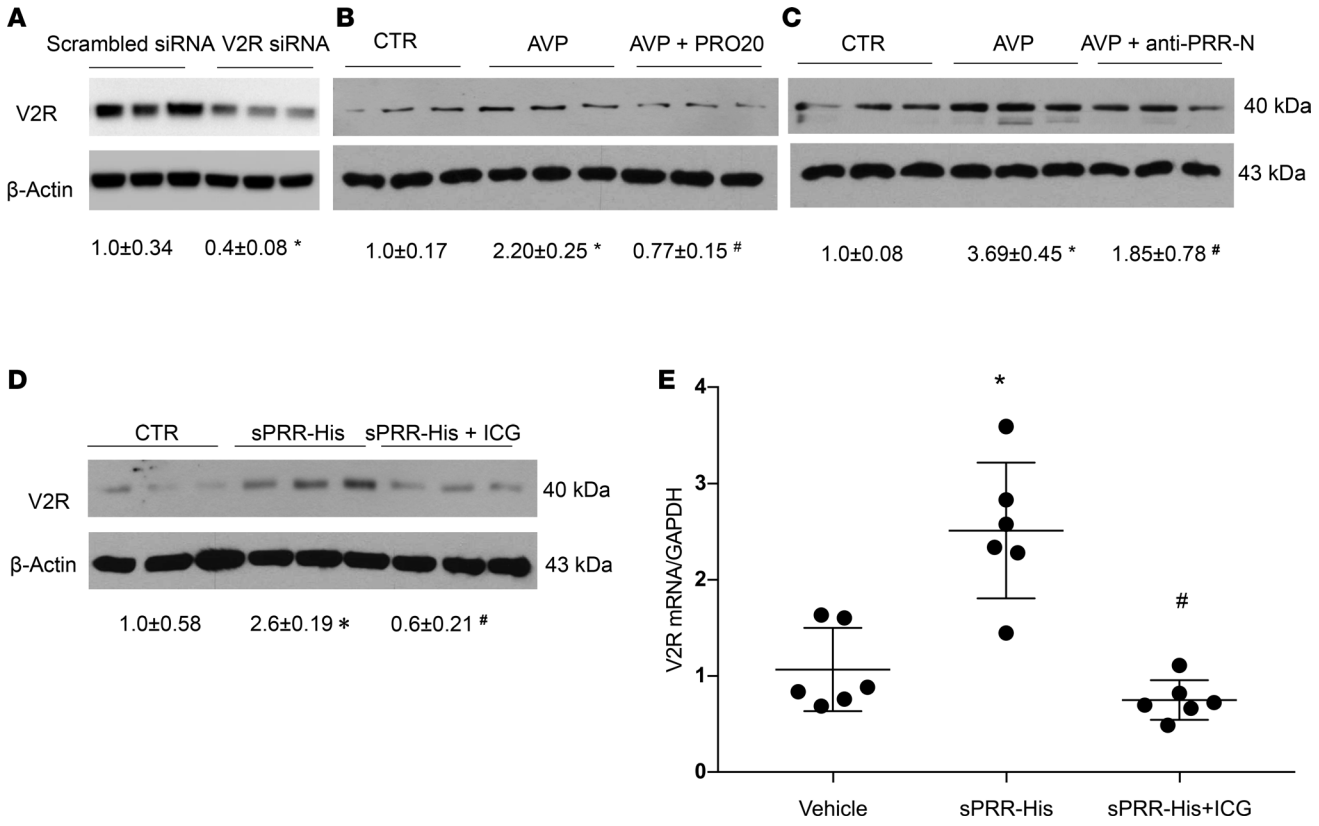

Figure 1. PRR-mediated AVP upregulation of V_2R expression in primary rat IMCD cells. The IMCD cells were pretreated with PRO20 or anti–PRR-N antibody and then treated for 24 hours with 10 nM AVP. V_2R protein expression was determined by immunoblotting and normalized by β-actin. (**A**) The validation of anti-V_2R antibody by using V_2R siRNA (n = 3 per group). (**B**) Effect of AVP alone or in combination with PRO20 on V_2R expression (n = 6 per group). (**C**) Effect of AVP alone or in combination with anti–PRR-N antibody on V_2R expression (n = 6 per group). In another experiment, primary rat IMCD cells were pretreated with a β-catenin inhibitor, ICG001 (ICG), and then treated for 24 hours with 10 nM sPRR-His. V_2R protein expression was determined by immunoblotting and qPCR and was normalized by β-actin and GAPDH, respectively. (**D**) Effect of sPRR-His alone or in combination with ICG on V_2R protein expression (n = 6 per group). (**E**) Effect of sPRR-His alone or in combination with ICG on V_2R mRNA expression (n = 6 per group). Statistical significance was determined by using unpaired Student's t test. Data are means ± SEM. CTR, control. $^*P < 0.05$ versus control; $^{\#}P < 0.05$ versus AVP or sPRR-His alone.

cells to regulate water reabsorption (16). Understanding the biological function of endogenous sPRR will be facilitated by the discovery of PRR cleaving protease. Earlier studies showed that the cleavage process depended on furin or ADAM19 (17, 18). However, recent studies by Nakagawa et al. (19) and our laboratory (20) using different approaches consistently demonstrate that site-1 protease (S1P) functions as a predominant source of sPRR production. In the present study, we attempted to define the role of S1P-derived sPRR in regulation of fluid homeostasis and to study the underlying mechanism involving V_2R regulation.

Results

In vitro investigation of S1P-derived sPRR in regulation of V_2R expression in cultured IMCD cells. The V_2R receptor is localized to the basolateral membrane of the CD principal cells and is responsible for elevating intracellular cAMP, thus increasing water permeability (21). V_2R expression in the CD cells is shown to be upregulated by AVP (22), in addition to hyperosmolality (23) and low pH (24). We attempted to examine PRR as a potential mediator of AVP regulation of V_2R expression in primary cultures of rat inner medullary collecting duct (IMCD) cells. IMCD cells were isolated from the inner medulla of SD rats and grown in 6-well plates. After reaching confluence, the cells were exposed to AVP in the presence or absence of a PRR antagonist PRO20 or anti–PRR-N antibody. By immunoblotting, the V_2R was detected as a single 40-kDa band. The specificity of the anti-V_2R antibody was validated by siRNA-mediated knockdown of V_2R mRNA (Figure 1A). Exposure to 100 nM AVP for 24 hours elevated the protein abundance of V_2R (Figure 1B). The increase in V_2R protein abundance was abolished by a PRR antagonist PRO20 (Figure 1B). The same result was obtained by using anti–PRR-N antibody as a PRR-neutralizing agent (Figure 1C).

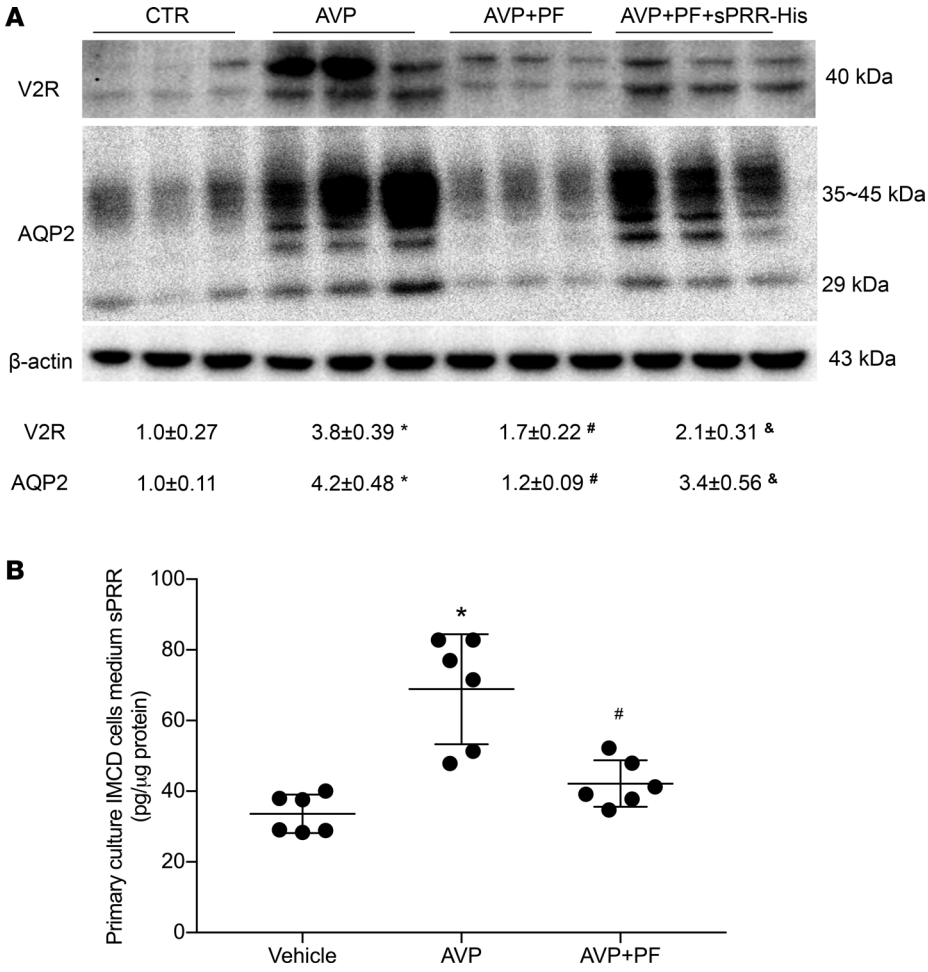

Figure 2. Effect of S1P inhibition alone or in combination with sPRR-His on AVP-induced V_2R and AQP2 expression in the CD cells. Primary rat IMCD cells were pretreated with PF alone or in combination with sPRR-His and then treated for 24 hours with 10 nM AVP. The expression of V_2R and AQP2 were analyzed by immunoblotting. Medium sPRR concentration was determined by using ELISA and normalized by protein content. (**A**) Immunoblotting analysis of V_2R and AQP2 expression (n = 3 per group). Densitometry values are shown underneath the blots. (**B**) ELISA analysis of medium sPRR content (n = 6 per group). Statistical significance was determined by using 1-way ANOVA with the Bonferroni test for multiple comparisons. $^*P < 0.05$ versus control (CTR); $^{\#}P < 0.05$ vs. PF-429242 alone, $^{\&}P < 0.05$ vs. AVP.

These results suggest involvement of PRR in mediating upregulation of V_2R expression by AVP.

A recombinant histidine-tagged rat sPRR was generated using a mammalian cell expressing system and termed sPRR-His (16). We examined the effect of sPRR-His on V_2R expression in primary IMCD cells. Following 24-hour exposure to 10 nM sPRR-His, V_2R protein expression was significantly increased as evaluated by immunoblotting (Figure 1D). Quantitative PCR (qPCR) detected a similar stimulation of V_2R mRNA in response to sPRR-His treatment (Figure 1E). In our previous study, we reported that sPRR signals via the β-catenin pathway to increase AQP2 expression in cultured ICMD cells (16). Therefore, we examined involvement of β-catenin signaling in V_2R regulation by sPRR-His. We found that a β-catenin inhibitor ICG001 effectively attenuated sPRR-His–induced V_2R protein and mRNA expression (Figure 1, D and E). These results suggest that PRR induces V_2R expression via sPRR activation of β-catenin signaling.

Recent reports from our group and others have identified S1P as a predominant protease responsible for the generation of sPRR (19, 20). Therefore, we examined the role of S1P-derived sPRR in mediating AVP upregulation of V_2R expression in primary rat IMCD cells. Following exposure for 24 hours to 10 nM AVP treatment, these cells exhibited a significant increase in V_2R protein expression, which was almost completely abolished by a S1P inhibitor PF-429242 (PF) (Figure 2A). The inhibitory effect of PF on V_2R expression was largely restored by adding sPRR-His (Figure 2A). AQP2 protein abundance was detected

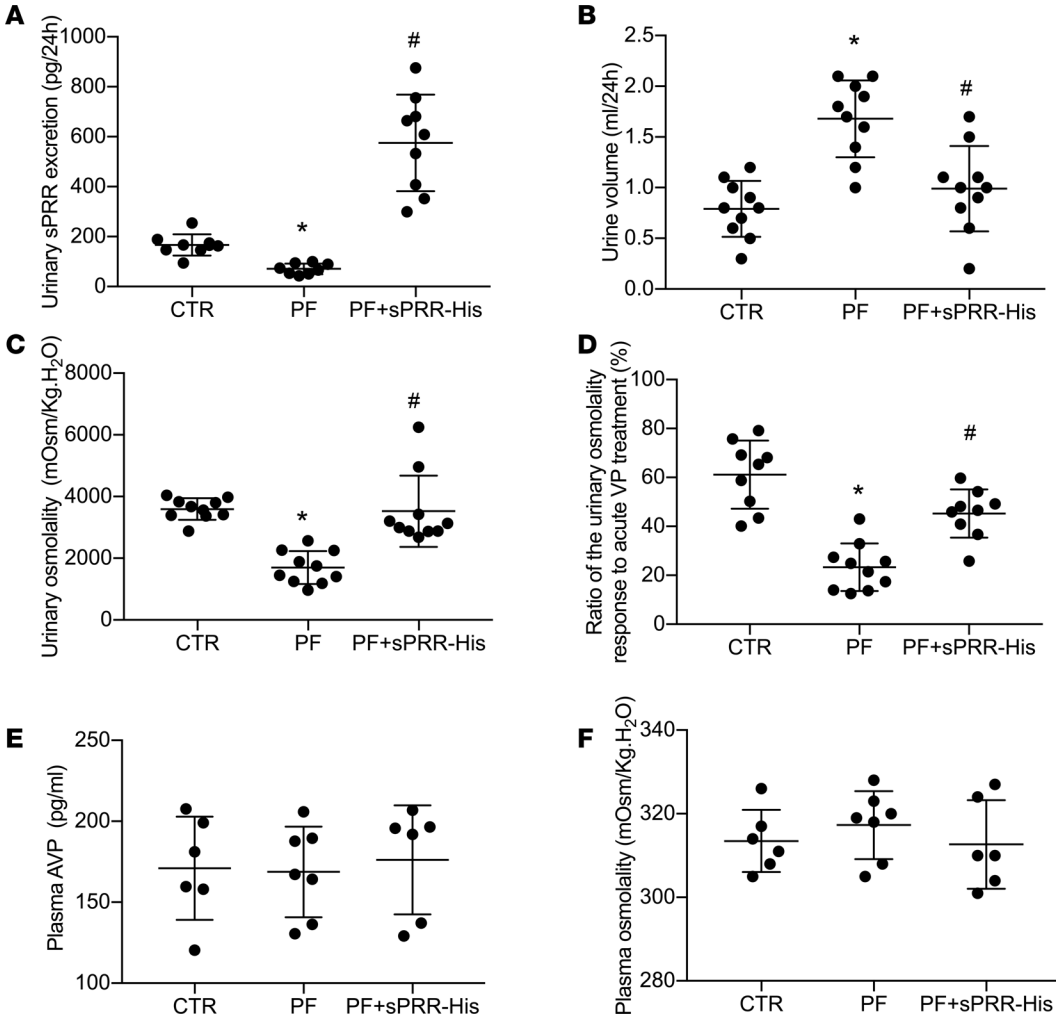

Figure 3. In vivo characterization of the diuretic action of S1P inhibition in C57/BL6 mice. Male C57/BL6 mice received s.c. infusion of a S1P inhibitor, PF-429242 (PF), with or without sPRR-His infusion for 4 days. The mice receiving vehicle treatment served as control. At the end of the experiment, 24-hour urine collection was performed, followed by ELISA analysis of urinary sPRR excretion. (**A**) ELISA analysis of urinary sPRR excretion (n = 10 mice per group). (**B**) Urine volume (n = 10 mice per group). (**C**) Urinary osmolality (n = 10 mice per group). (**D**) Analysis of urine osmolality response to acute AVP treatment (n = 10 mice per group). (**E**) ELISA analysis of plasma AVP concentration (n = 6 mice per group). (**F**) Plasma osmolality (n = 6 mice per group). Statistical significance was determined by using 1-way ANOVA with the Bonferroni test for multiple comparisons. $^{*}P < 0.05$ vs. control; $^{\#}P < 0.05$ vs. PF alone.

on the stripped blot and exhibited a similar pattern as V_2R expression (Figure 2A). Medium sPRR, which was detected by ELISA, was elevated by AVP and suppressed by PF (Figure 2B).

Pharmacological investigation of the role of S1P-derived sPRR in regulation of water homeostasis in mice. To test the role of S1P-derived sPRR in regulation of water homeostasis, we administered PF alone or in conjunction with sPRR-His to C57/BL6 mice. Urinary sPRR was reduced by PF and was increased several-fold following sPRR-His infusion (Figure 3A). PF mice displayed polyuria and hypoosmotic urine, both of which were nearly completely reversed by sPRR-His infusion (Figure 3, B and C). The magnitude of changes in urinary osmolality in response to acute AVP treatment was taken as an index of AVP sensitivity. PF blunted AVP sensitivity, and this effect was reversed by sPRR infusion (Figure 3D) without affecting the plasma AVP level, osmolality (Figure 3, E and F), Na^+, or K^+ (data not shown). Immunoblotting demonstrated that PF infusion induced a parallel reduction of protein abundance of V_2R, AQP2, and NKCC2 (Figure 4, A and B). Interestingly, sPRR-His infusion restored the expression of V_2R and AQP2 but not NKCC2 (Figure 4, A and B). The results suggested that the pharmacological inhibition of S1P influenced V_2R/AQP2 and NKCC2 expression via distinct mechanisms depending on involvement of sPRR.

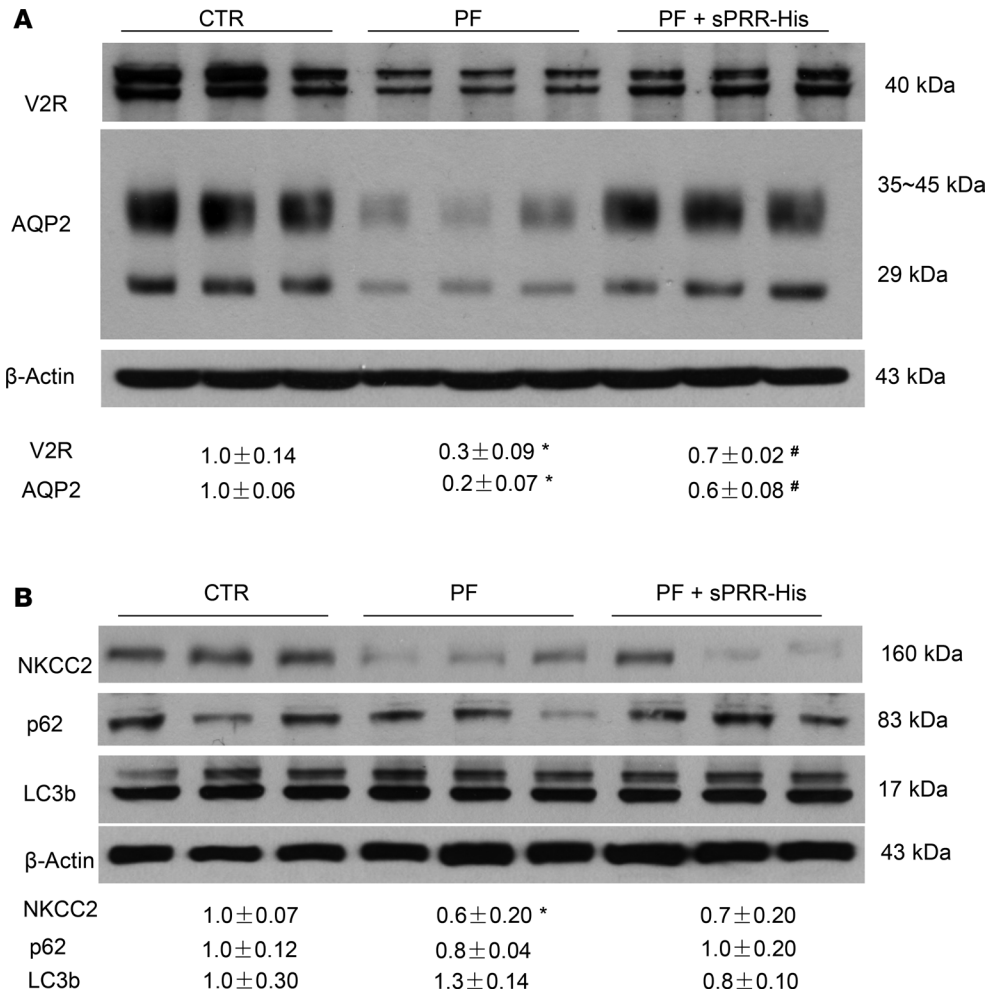

Figure 4. Effect of SIP inhibition alone or in combination with sPRR-His on renal expression of V_2R, transporter proteins, and autophagosome markers in C57/BL6 mice. Male C57/BL6 mice were treated with vehicle, PF alone, or in combination with sPRR-His. The renal expression of V_2R, AQP2, NKCC2, and the markers of autophagosome (p62 and LC3b) was analyzed by immunoblotting. (**A**) Immunoblotting analysis of V_2R and AQP2 expression (n = 8 mice per group). (**B**) Immunoblotting analysis of NKCC2, p62, and LC3b expression (n = 8 mice per group). Densitometry values are shown underneath the blots. Statistical significance was determined by using unpaired Student's t test. $^*P < 0.05$ versus control (CTR); $^{\#}P < 0.05$ vs. PF-429242 alone.

Trepiccione et al. report that Renal tubular PRR KO (RT PRR–KO) mice exhibit a strong autophagic defect in medullary epithelial cells, as characterized by accumulation of autophagosome markers, including p62 and microtubule-associated protein 1A/1B-light chain 3 (LC3b), in the TAL and to less extent in the CD (12). Such an autophagic abnormality has been proposed as a potential mechanism to explain the downregulation of NKCC2, as well as AQP2 expression in the RT PRR–KO mice (12). Accordingly, we examined whether S1P inhibition affected expression of the same autophagosome markers. To our surprise, the protein expression of microtubule-associated LC3b or p62 was unaffected by either PF or sPRR-His (Figure 4B). These results revealed no evidence for sPRR regulation of renal autophagy under the current experimental condition.

Generation of RT S1P–KO mice and analysis of the phenotype during regulation of water homeostasis. Inducible renal tubule–wide deletion of S1P was created by crossing $S1P^{fl/fl}$ mice with Pax8/LC1 transgenic mice, followed by doxycycline treatment in the adult animals. This method was originally developed by Trykova-Brauch et al. (25) and later validated by multiple investigators (10, 12, 26). As expected, a PCR-based strategy showed DNA recombination in the kidney and liver but not other organs (Figure 5, A–C). By immunoblotting, renal protein abundance of S1P was decreased in $S1P^{fl/+}$-Cre^+ mice as compared with $S1P^{fl/+}$-Cre^- controls, and the reduction was more obvious in $S1P^{fl/fl}$-Cre^+ mice following

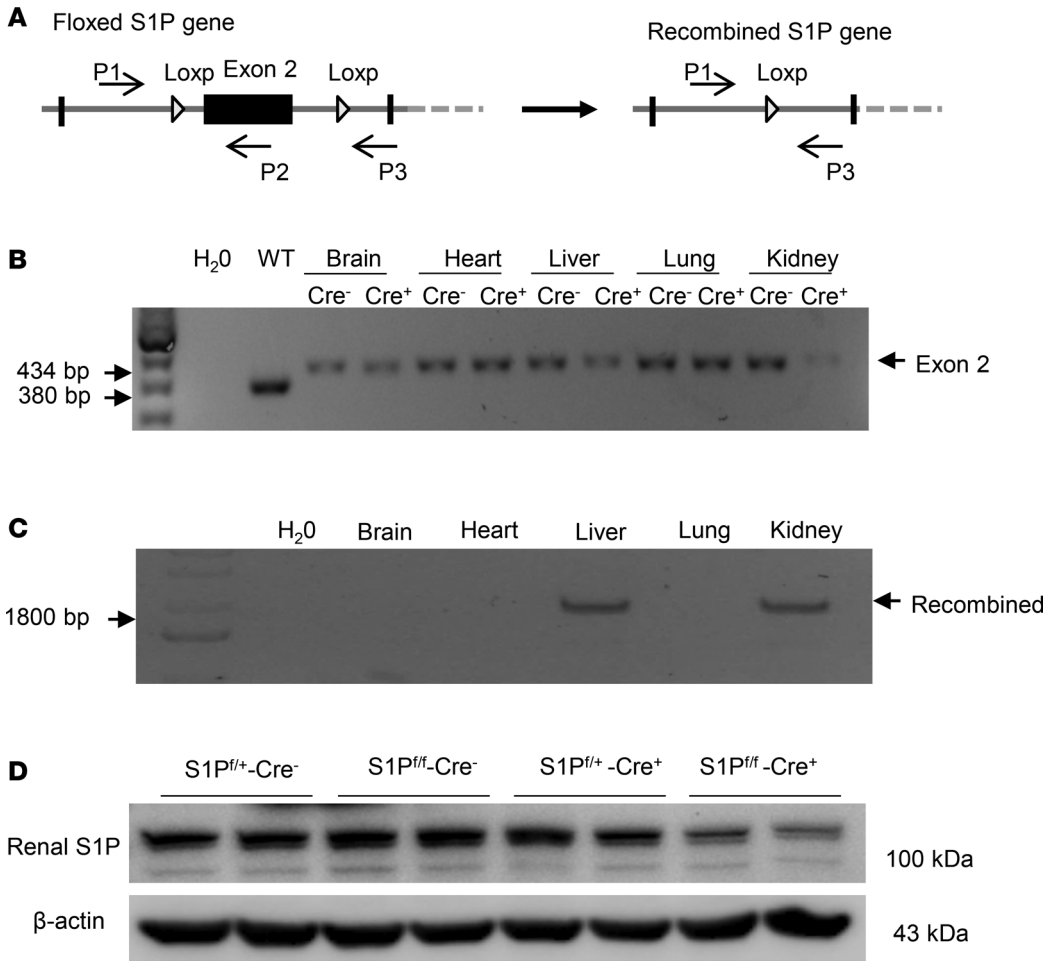

Figure 5. Validation of inducible renal tubule–specific deletion of S1P. (**A**) Schematic illustration of the PCR strategy to detect the floxed and recombined alleles by using primers P1 × P2 and P1 × P3, respectively. (**B**) PCR amplification using P1 × P2 to detect the floxed allele from various organs of $S1P^{fl/fl}$-Cre^+ and $S1P^{fl/fl}$-Cre^- mice following doxycycline treatment. WT denotes C57/BL6 mouse. This amplification resulted in a 434-bp product from the floxed allele and a 380-bp product from WT allele. (**C**) PCR amplification using P1 × P3 to detect the recombined allele from various organs of $S1P^{fl/fl}$-Cre^+ following doxycycline treatment. The recombined allele was detected as an 1800-bp product. (**D**) Confirmation of renal S1P deletion at protein level. Immunoblotting analysis of renal S1P protein expression in mice with the indicated genotypes following the same doxycycline treatment.

doxycycline treatment (termed as RT S1P–KO mice) (Figure 5D). The null mice were grossly indistinguishable from their floxed controls. However, under basal conditions, the null mice at the age of 10–12 weeks developed polyuria, hypoosmotic urine, and blunted AVP response, which were all significantly attenuated by administration of sPRR-His (Figure 6, A–C). By immunoblotting, RT S1P–KO mice had parallel reductions of renal protein expression of V_2R, AQP2, and NKCC2 as compared with the floxed controls (Figure 7). Interestingly, sPRR-His infusion restored the expression of V_2R and AQP2 but not NKCC2 (Figure 7). Therefore, the phenotype of RT S1P–KO mice is largely reminiscent of the original observation from the pharmacological investigation.

The rescue of the DI phenotype in PRR-null mice by sPRR-His. Our previous studies have shown that conditional deletion of PRR from the renal tubules (RT PRR–KO) or the CD (CD PRR–KO) induced severe polyuria, hypoosmotic urine, accompanied by a significant reduction of renal AQP2 protein expression (13, 27). However, whether this phenotype was due to reduced sPRR production was unclear. Furthermore, whether sPRR acted through V_2R remains uninvestigated, although it has been shown to upregulate AQP2 expression in cultured CD cells (28). We first analyzed V_2R expression in the renal medulla of RT PRR–KO and CD PRR–KO mice under basal conditions. By immunoblotting, renal medullary V_2R protein abundance was reduced by 60% in CD PRR–KO mice (Figure 8A) and by 75%

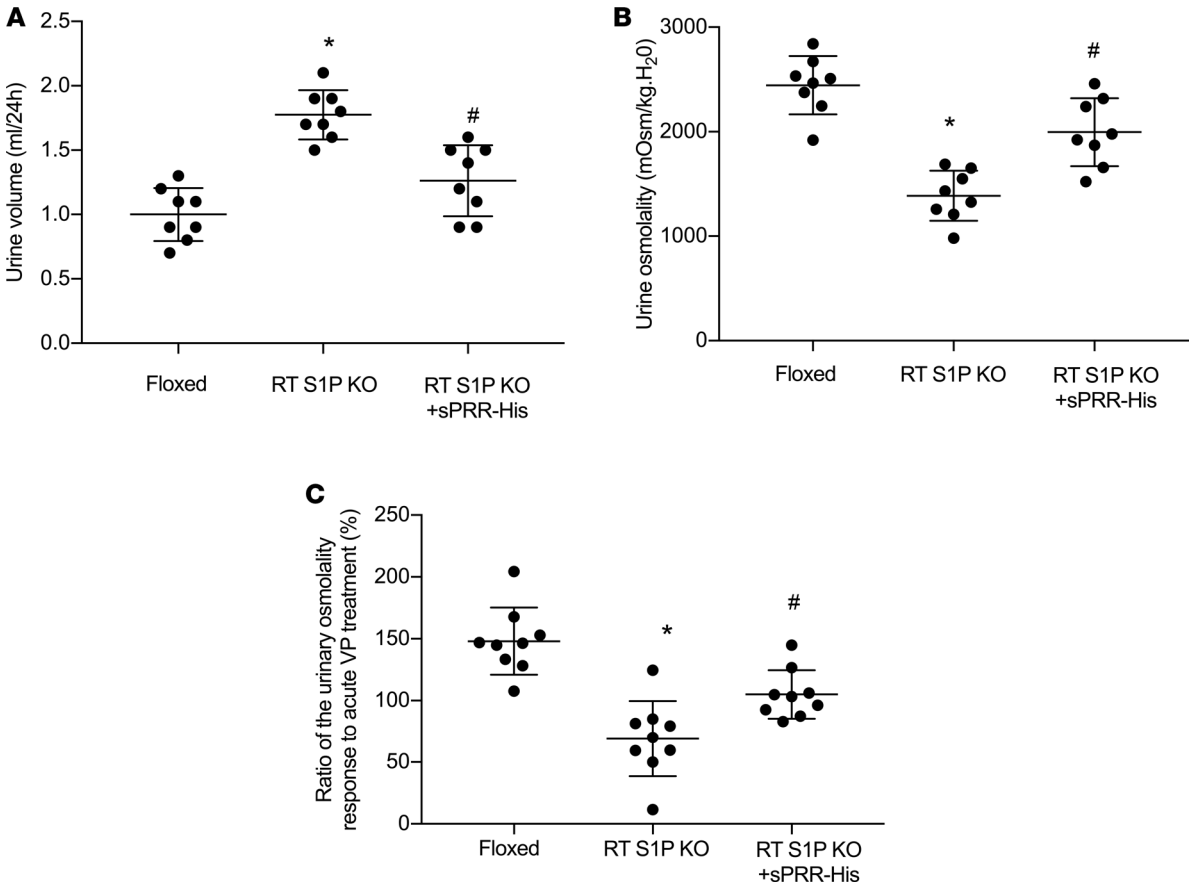

Figure 6. Analysis of fluid homeostasis in RT S1P–KO mice and rescue of the phenotype with sPRR-His. At the age of 3–4 months, RT S1P–KO mice were infused with vehicle or sPRR-His infusion via osmotic minipump at 30 μg/kg/day for 7 days. At the end of the experiments, 24-hour urine collections were performed and urine osmolality response to acute AVP injection was determined. (**A**) Urine volume (n = 8 mice per group). (**B**) Urine osmolality (n = 8 mice per group). (**C**) Ratio of the change in urine osmolality response to acute AVP treatment. Urine was emptied by bladder massage and subjected to measurement of osmolality before and after AVP (720 ng/kg body weight) treatment (n = 8–9 mice per group). Statistical significance was determined by using 1-way ANOVA with the Bonferroni test for multiple comparisons. Data are mean ± SEM. *P < 0.05 vs. control; #P < 0.05 vs. RT S1P–KO mice alone.

in RT PRR–KO mice (Figure 8C). In parallel, renal medullary V_2R mRNA expression, as assessed by qPCR, was reduced by 52% in CD PRR–KO mice (Figure 8B) and by 58% in RT PRR–KO mice (Figure 8D). Subsequently, we administered sPRR-His to the 2 strains of null mice. Baseline urinary sPRR excretion, as assessed by ELISA, was reduced by 28% in CD PRR–KO mice and 73% in RT PRR–KO mice (Figure 9, A and B); following sPRR-His infusion, urinary sPRR increased several-fold in both PRR-null groups. Under basal conditions, CD PRR–KO mice developed a modest degree of DI, as previously described (urine volume [UV]: KO, 2.2 ± 0.4, versus floxed, 1.2 ± 0.3 ml/d;P<0.05; ref. 19). A 3-day sPRR-His infusion in CD PRR–KO mice significantly attenuated the polyuria and improved urine osmolality (Figure 9, C and D). In contrast, RT PRR–KO mice developed more robust polyuria (~6-fold) and hypotonic urine (Figure 9, E and F). The antidiuretic action of sPRR-His was similarly observed in RT PRR–KO mice, albeit with a slower or incomplete response. The significant effect of sPRR-His in RT PRR–KO mice was not observed until day 7 and was maximal at day 10. In both null strains, sPRR-His infusion significantly elevated renal medullary protein abundance of both V_2R and AQP2 (Figure 10A). Besides the abnormality in the V_2R-AQP2 axis, RT PRR–KO mice also exhibited suppressed NKCC2 protein expression (Figure 10B). In contrast, the downregulation of NKCC2 was unaffected by sPRR-His infusion (Figure 10B).

Next, we reexamined the issue concerning the potential relationship between PRR/sPRR and the autophagasome accumulation. As expected, RT PRR–KO mice displayed a remarkable upregulation of autophagosome markers, including p62 and LC3b (Figure 10B), as previously reported by Trepiccione et al. (12). However, neither of these markers was affected by sPRR-His infusion (Figure 10B). Interestingly, unlike

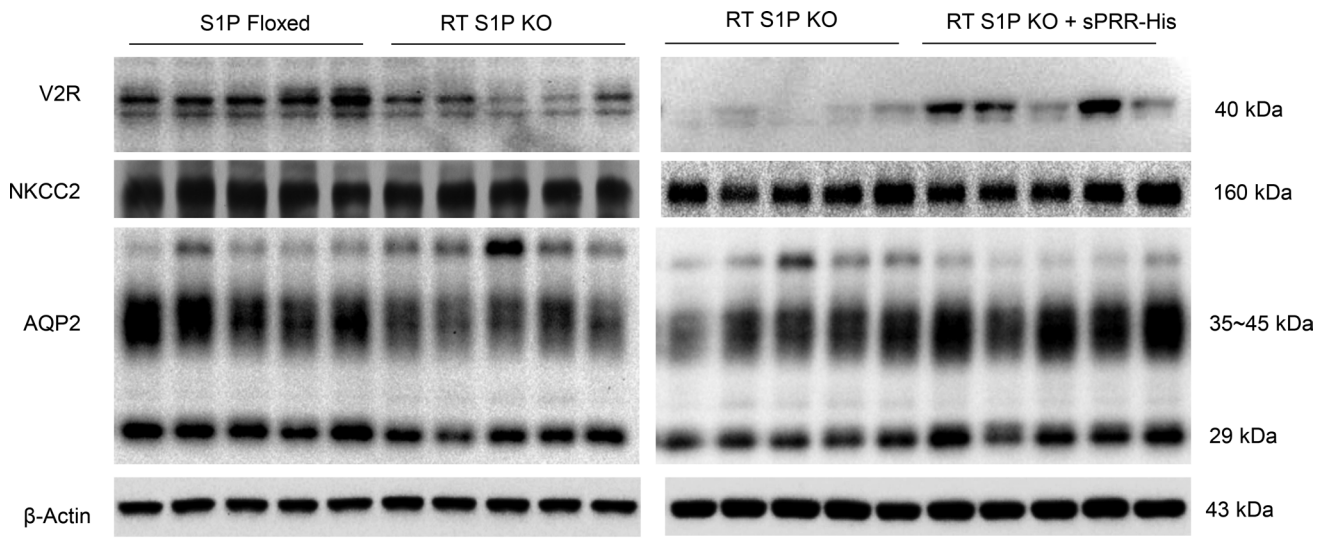

V2R	1.0±0.14	0.4±0.16 *	1.0±0.12	3.7±0.40 #
NKCC2	1.0±0.11	0.9±0.12	1.0±0.22	0.8±0.26
AQP2	1.0±0.24	0.3±0.17 *	1.0±0.39	4.6±0.34 #

Figure 7. Analysis of renal expression of V_2R and transporters in RT S1P–KO mice following sPRR-His infusion. Renal expression of V_2R, NKCC2, and AQP2 was analyzed by immunoblotting analysis. The left panels show the baseline values between the genotypes. The right panels show the changes in the null mice following sPRR-His infusion. The densitometry values were normalized by β-actin and shown underneath the blots. Of note, for a better comparison between 2 groups, the protein samples from the RT S1P–KO group were from the same animals. Statistical significance was determined by using unpaired Student's *t* test. $^*P < 0.05$ versus floxed; $^{\#}P < 0.05$ vs. RT S1P–KO mice.

RT PRR–KO mice, CD PRR–KO mice did not have elevated expression of p62 or LC3b (data not shown). These results suggest that autophagosome accumulation induced by PRR deletion may occur primarily in the TAL but not in the CD, which can be dissociated from the antidiuretic action of sPRR-His.

CD PRR–KO mice had a 42% reduction of baseline AVP sensitivity, which was almost completely normalized following a 3-day sPRR-His infusion (Figure 11A). A relatively greater reduction of baseline AVP sensitivity was observed in RT PRR–KO mice, in parallel with more severe DI phenotype. sPRR-His infusion over a longer period of time induced a partial but significant restoration of AVP sensitivity in RT PRR–KO mice (Figure 11B).

Besides the peripheral tissues, PRR is also expressed in the CNS, particularly the neurons secreting AVP (29). Indeed, evidence is available to suggest a functional role of PRR in regulation of central AVP production and, thus, urine concentrating capability, as well as blood pressure (29). However, no prior report examines the involvement of sPRR in regulation of AVP production. We therefore performed ELISA to measure urinary AVP excretion in our models. Twenty-four hour urinary excretion of AVP was unaffected in both strains of the null mice, irrespective of sPRR-His infusion (Figure 11, C and D). These results support the concept that sPRR selectively targets the V_2R-AQP2 axis in the CD without affecting central AVP production.

Discussion

Compelling evidence from pharmacologic and conditional gene KO studies has established a crucial role for PRR in determining renal AQP2 expression and urine concentrating capability (30, 31). In particular, mice lacking PRR from the renal tubule or the CD consistently developed severe DI associated with a remarkable downregulation of AQP2 expression (16, 27). Our previous study further demonstrates that exogenous sPRR exerts a biological function in regulation of AQP2 expression and urine concentrating capability (16). Recently, S1P — but not furin or ADAM19 — has shown to be the predominant source of sPRR generation. In the present study, we provide pharmacological and genetic evidence to support an essential role of S1P-derived sPRR in regulation of fluid homeostasis, and we further identify V_2R as its molecular target.

V_2R is the principal receptor subtype responsible for antidiuretic action of AVP (32). It is localized to the basolateral membrane of the principal cells of the CD. As a Gs-coupled GPCR, V_2R activation by AVP leads to increased intracellular cAMP and, thus, activation of protein kinase A (PKA), which induces trafficking of

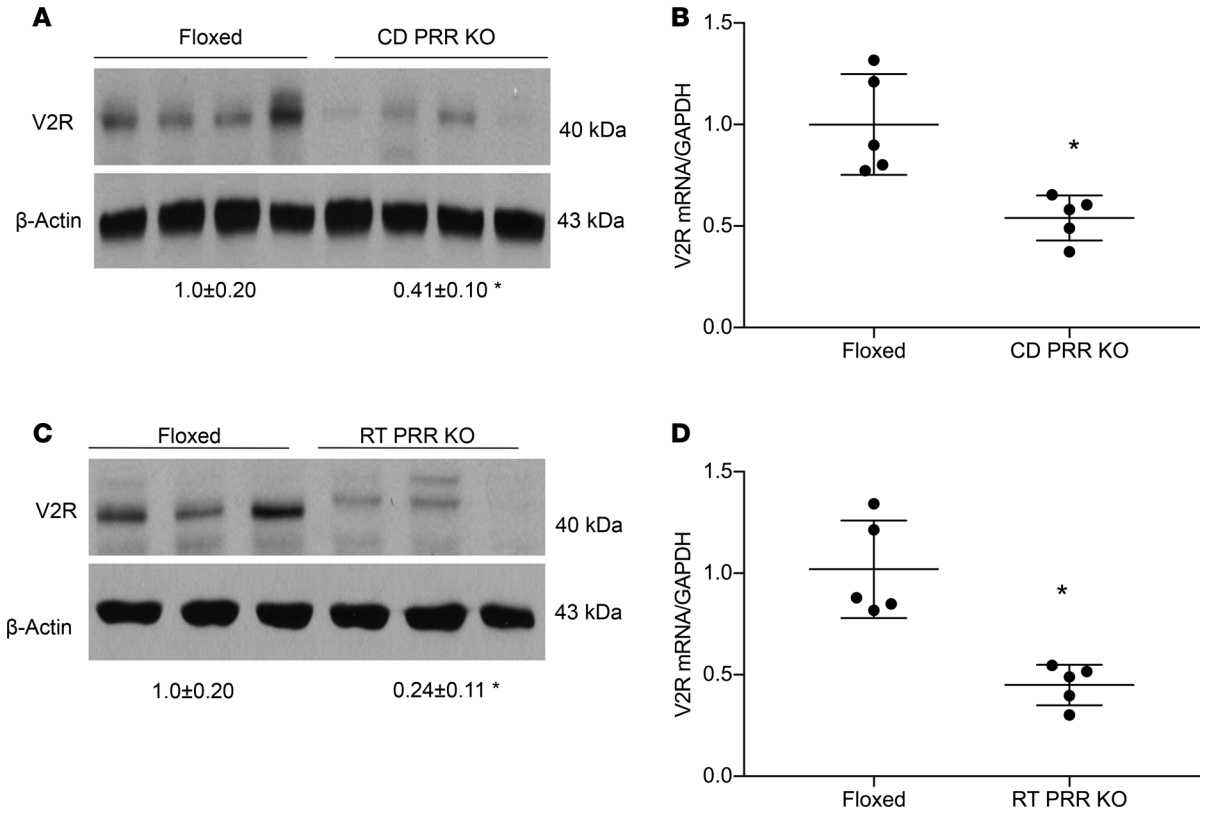

Figure 8. Analysis of renal V_2R expression in PRR-KO mice. Under basal conditions, the kidneys of CD PRR–KO and RT PRR–KO mice and their respective floxed controls were harvested and analyzed for V_2R expression. (**A** and **C**) Immunoblotting analysis of renal V_2R expression. (**B** and **D**) qPCR analysis of V_2R mRNA expression (n = 5 mice per group). Statistical significance was determined by using unpaired Student's t test. Data are means ± SEM. *$P < 0.05$ versus floxed.

AQP2 to the apical membrane and enhancement of water permeability in the CD (1, 33). While the AQP2 trafficking process has been well delineated, less is known about the regulation of V_2R, a key determinant of the antidiuretic action of AVP. In the present study, we report for the first time to our knowledge that sPRR functions as an important regulator of renal V_2R expression. In vitro data showed that V_2R expression was elevated following exposure to sPRR-His. The stimulation of V_2R expression by sPRR is mediated by β-catenin signaling, since it is blocked by ICG001, an inhibitor of β-catenin signaling. We previously reported that sPRR signals through β-catenin to induce AQP2 expression (16). Consistent with the in vitro observation, compelling in vivo data demonstrate sPRR as a regulator of renal V_2R expression. At basal condition, renal mRNA and protein expression of V_2R is consistently suppressed in mice lacking PRR in the CD or renal tubules. At functional level, AVP sensitivity is also consistently impaired in both PRR-null strains. It is likely that defective V_2R, at least in part, accounts for the suppressed renal AQP2 expression and urine concentrating capability induced by renal tubule– and CD-specific deletion of PRR. We provide further evidence that the V_2R regulatory role of PRR is mediated by sPRR. In this regard, urinary excretion of sPRR is reduced in both strains of PRR-null mice. More importantly, the polyuria phenotype, renal expression of V_2R and AQP2, in the null mice were all rescued by administration of sPRR-His. Together, these data support the concept that sPRR directly regulates renal V_2R expression via β-catenin signaling, thus controlling AVP sensitivity. In addition, sPRR signals through the same β-catenin pathway to independently stimulate AQP2 transcription (16). Thus, sPRR is an effective regulator of renal AVP-V_2R-AQP2 axis owing to its capability to simultaneously target both V_2R and AQP2. In agreement with the current study, the cAMP response to AVP is blunted in MDCK.C11 cells transfected with PRR siRNA (34) as well as in isolated renal medullary CDs (35).

Besides the CD, the TAL is another important site of antidiuretic action of AVP (5, 36, 37). This nephron site accounts for 30% NaCl reabsorption via furosemide-sensitive NKCC2–mediated active NaCl transport and is water impermeable; it therefore serves to maintain the longitudinal osmotic gradient and promote efficient water reabsorption in the CD. As in the CD, the AVP-V_2R axis is also operative in the

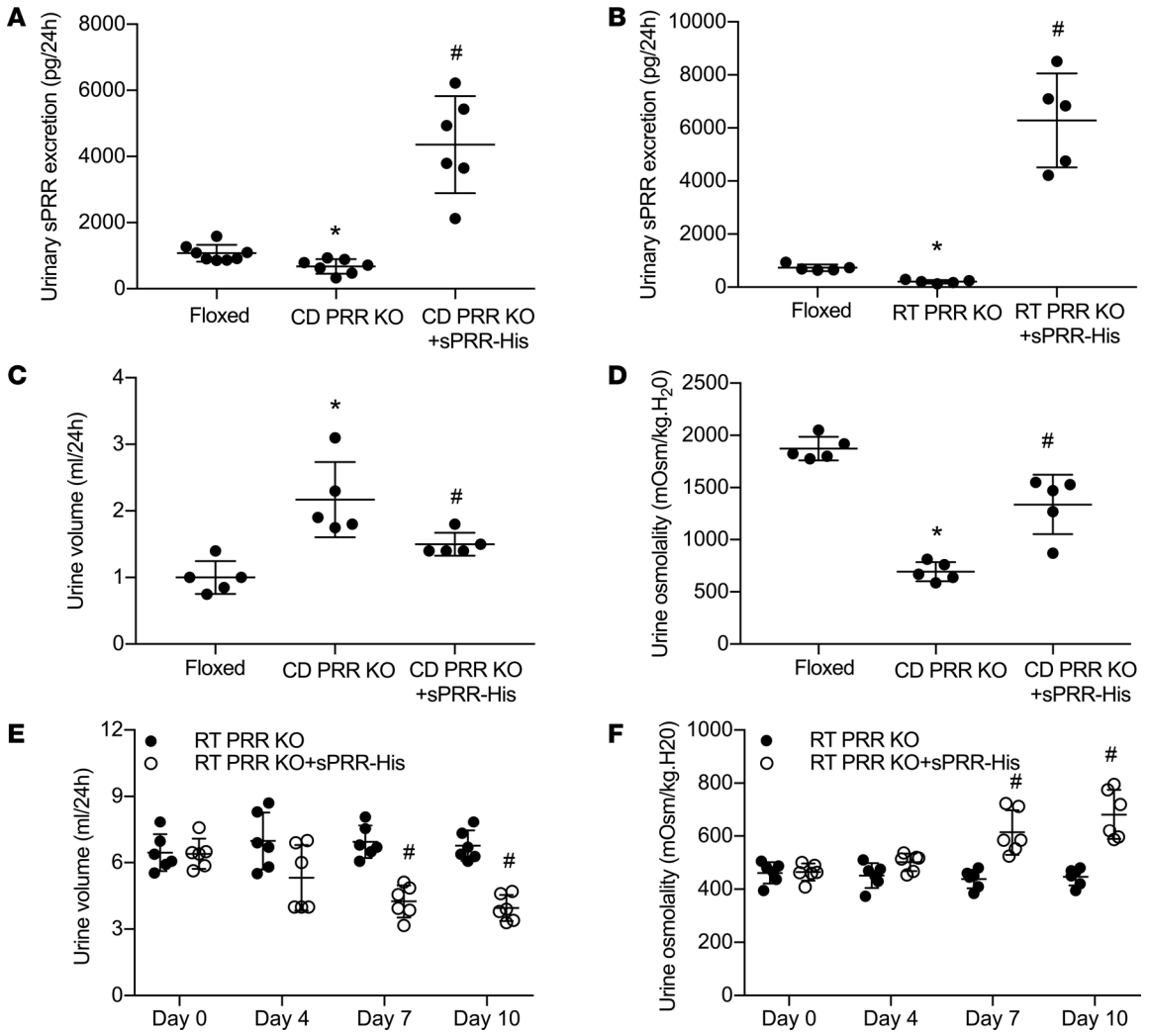

Figure 9. Effect of sPRR-His infusion on urine concentrating capability in PRR-KO mice. CD PRR–KO and RT PRR–KO mice were given sPRR-His infusion at 30 μg/kg/day for 4 and 7 days, respectively. At the end of the experiments, 24-hour urine collections were performed. (**A** and **B**) ELISA determination of urinary sPRR excretion (n = 5–8 mice per group). (**C**) Urine volume in CD PRR–KO mice (n = 5 mice per group). (**D**) Urine osmolality in CD PRR–KO mice (n = 5 mice per group). (**E**) Urine volume in RT PRR–KO mice (n = 6 mice per group). (**F**) Urine osmolality in RT PRR–KO mice (n = 6 mice per group). Statistical significance was determined by using 1-way ANOVA with the Bonferroni test for multiple comparisons. Data are mean ± SEM. *P < 0.05 vs. control; #P < 0.05 vs. PRR KO mice alone.

TAL via releasing intracellular cAMP to activate PKA (36). In the TAL, the stimulation of AVP-V_2R axis induces phosphorylation of NKCC2 at several conserved NH2-terminal threonine and serine residues to increase its activity (5, 6). The functional contribution of AVP signaling in the TAL has recently been elegantly tested by using transgenic rats expressing a dominant negative V_2R mutant (Ni3-Glu242stop) under the control of Tamm-Horsfall protein (THF) promoter (5). The TAL-specific inactivation of V_2R results in significant polyuria under basal conditions and failure to concentrate urine following water deprivation, associated with reduced renal expression of NKCC2 and p-NKCC2. Therefore, V_2R-dependent activation of NKCC2 in the TAL is a prerequisite for the overall urine concentrating capability.

It is not surprising that, as an effective regulator of urine concentrating capability, PRR targets NKCC2 in addition to AQP2. Indeed, renal NKCC2 expression is significantly reduced in parallel with suppressed AQP2 expression in the RT PRR–KO mouse model (12). In agreement with this observation, we found that renal expression of both NKCC2 and AQP2 was reduced in RT PRR–KO mice. Likely due to suppression of NKCC2 and AQP2 expression, RT PRR–KO mice exhibited more severe polyuria as compared with CD PRR–KO mice. Interestingly, the 2 null strains responded to sPRR-His differently in terms of timeframe of alleviation of polyuria and the restoration of transporter proteins.

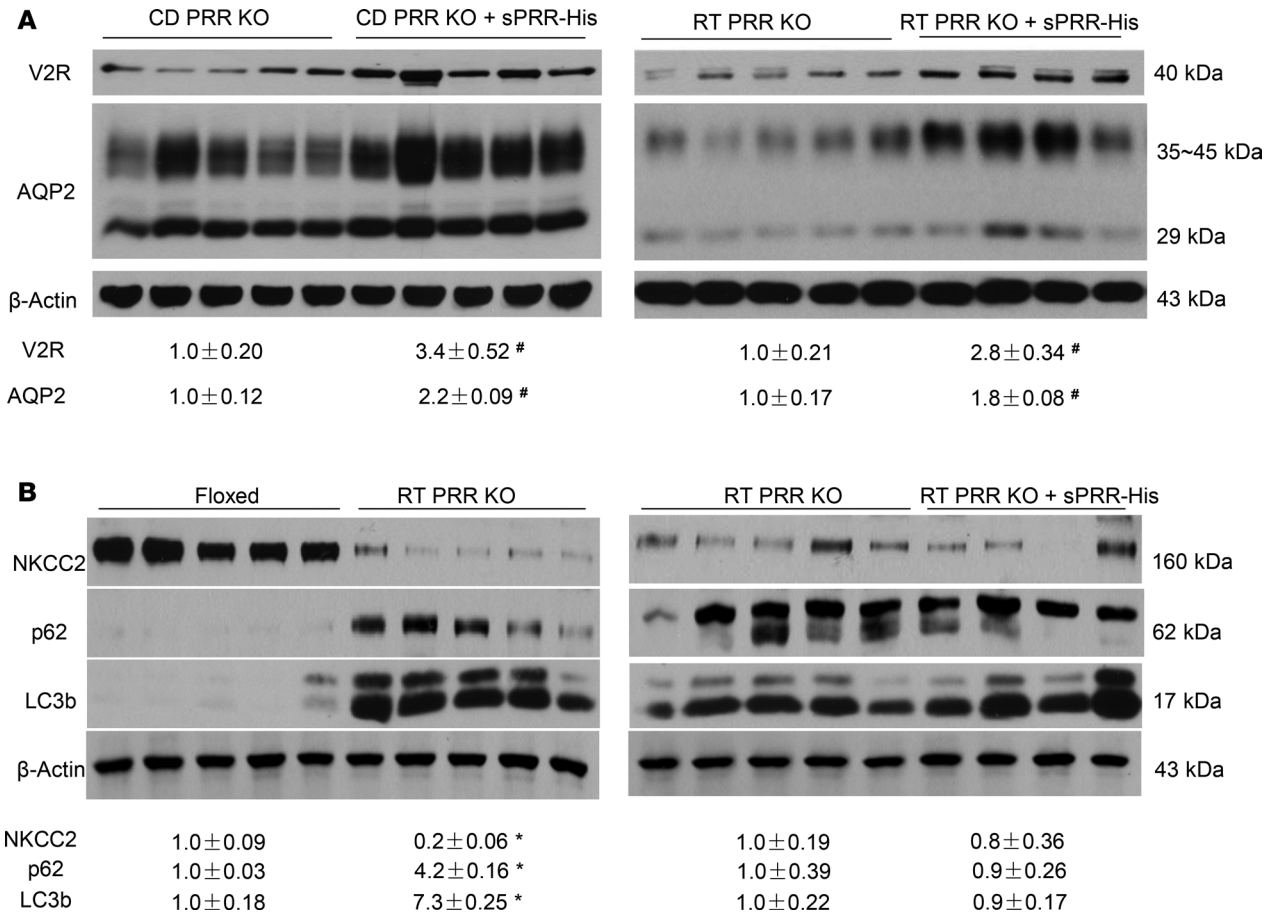

Figure 10. Analysis of renal expression of V_2R and transporters in PRR-KO mice following sPRR-His infusion. (**A**) Immunoblotting analysis of renal expression of V_2R and AQP2 in CD PRR–KO (left panel) and RT PRR–KO mice (right panel) with and without sPRR-His infusion. (**B**) Immunoblotting analysis of renal expression of NKCC2 and markers of autophagosome accumulation including p62 and LC3b in floxed and RT PRR–KO mice under basal conditions (left panel). The comparison of abundance of these proteins was made between RT PRR–KO/vehicle and RT PRR–KO/sPRR-His mice (right panel). The values were normalized by β-actin and shown underneath the blots. Statistical significance was determined by using unpaired Student's *t* test. **P* < 0.05 versus floxed; #*P* < 0.05 vs. PRR-KO mice.

The full antidiuretic action of sPRR-His occurred in CD PRR–KO mice at day 3, whereas a significant effect of sPRR-His in RT PRR-KO mice didn't happen until day 7. At a molecular level, the renal expression of V_2R and AQP2, but not NKCC2, was restored by sPRR-His in the null strains. These results strongly suggest that sPRR-His selectively affects V_2R-AQP2 axis in the CD but not the TAL. In light of intercalated cells as a major site of renal PRR expression, we propose a paracrine mechanism by which intercalated cell–derived sPRR acts on the apical membrane of principal cells to regulate AQP2-mediated water transport (16). This notion is reinforced by the current observation concerning a major antidiuretic action of sPRR in the CD.

Besides the physiological function of PRR in the kidney, PRR is well known to regulate development and integrity of multiple tissue types, as highlighted by pathological abnormalities and lethality induced by systemic or organ-specific deletion of PRR (38–40). In particular, RT PRR–KO mice develop prominent autophagosome accumulation in the TAL and, to a lesser extent, in the CD, which has been postulated to contribute to decreased expression of NKCC2, as well as AQP2 (12). However, our results don't support this speculation. In this regard, there was no correlation between renal AQP2 abundance and the markers of the autophagosome (p62 and LC3b) in RT PRR–KO mice in response to sPRR-His infusion. Furthermore, unlike RT PRR–KO mice, CD PRR–KO mice showed little evidence of autophagosome accumulation (data not shown).

S1P has recently been identified as a predominant protease responsible for generation of sPRR (19, 20). In the present study, we employed a S1P inhibitor and RT S1P–KO model to test the potential role of endogenous sPRR in regulation of fluid homeostasis. Under basal conditions, mice treated with PF

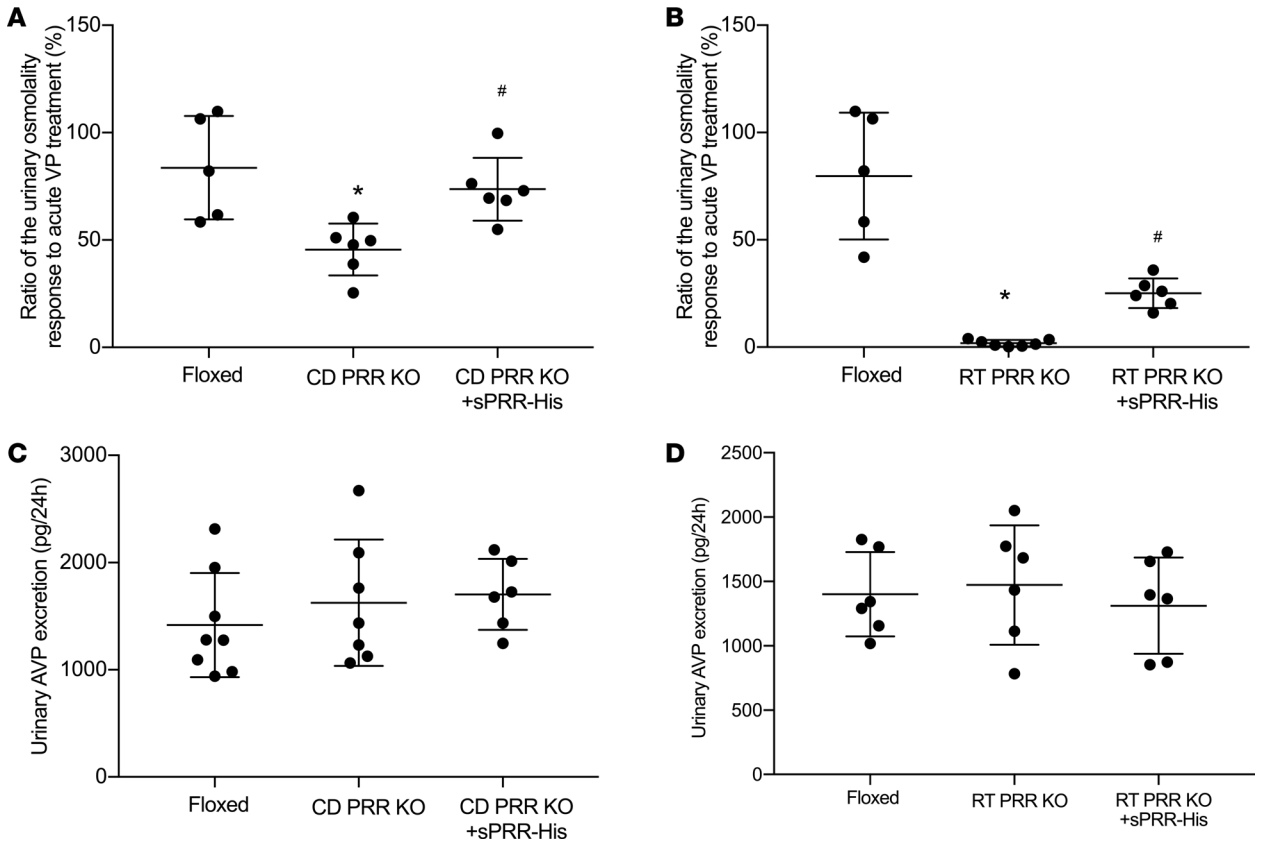

Figure 11. Effect of sPRR-His infusion on urine osmolality response to acute arginine vasopressin (AVP) treatment in PRR KO mice. Urine was emptied by bladder massage and subjected to measurement of osmolality before and after AVP treatment (720 ng/kg body weight). (**A** and **B**) Shown is the ratio of the change in urine osmolality in CD PRR–KO mice (n = 6 mice per group) (**A**) and RT PRR–KO mice (n = 6-7 mice per group) (**B**). (**C**) Twenty-four–hour urinary AVP excretion in floxed, CD PRR–KO/vehicle, and CD PRR–KO/sPRR-His mice (n = 6–8 mice per group). (**D**) Twenty-four–hour urinary AVP excretion in floxed, RT PRR–KO/vehicle,and RT PRR–KO/sPRR-His mice (n = 6 mice per group). Statistical significance was determined by using 1-way ANOVA with the Bonferroni test for multiple comparisons. Data are mean ± SEM. $^{*}P < 0.05$ vs. control; $^{\#}P < 0.05$ vs. PRR-KO mice alone.

displayed higher UV and lower urine osmolality — accompanied with decreased renal AQP2 and V_2R expression — and impaired AVP sensitivity, in parallel with reduced urinary sPRR excretion. Administration of sPRR-His nearly completely blocked PF-induced polyuria with significant restoration of V_2R and AQP2 expression. These results were recapitulated in RT S1P–KO mice. The consistent observation made by the pharmacological and genetic studies strongly supports a causal relationship between endogenous sPRR production and urine concentrating capability. Interestingly, not only did S1P inhibition affect the V_2R-AQP2 axis, but it also reduced NKCC2 expression. The mechanism for the downregulation of NKCC2 due to S1P inhibition remains unclear. This result may suggest a role of S1P-derived sPRR in regulation of NKCC2 expression. However, exogenous sPRR-His infusion doesn't affect NKCC2 expression in either PF-treated or RT PRR–KO mice. It seems reasonable to speculate that sPRR may act intracellularly in the TAL to control NKCC2 expression, in contrast to the extracellular action of sPRR in the CD. The distinct mechanisms of action of sPRR in the TAL versus the CD certainly warrant further investigation. It is also possible that S1P may regulate NKCC2 independently of sPRR. Besides PRR, S1P modifies unique membrane-bound latent transcription factors. A well-studied representative of this type of transcription factors is the sterol regulatory element–binding transcription factor (SREBP), a crucial transcription factor governing cholesterol and fatty acid biosynthesis (41–44). Similarly, S1P also processes membrane-bound activating transcription factor 6 (ATF6) during ER stress response (45). Currently, no evidence is available to our knowledge to suggest involvement of SREBP or ATF6 in regulation of urine concentrating capability. As discussed above, we found no association between sPRR-His and autophagosome accumulation. In support of this notion, suppression of endogenous sPRR production through S1P inhibition didn't influence the level of autophagy markers.

In conclusion, the present study has comprehensively investigated the role and mechanisms of sPRR in regulation of fluid homeostasis. We report that sPRR derived from S1P functions as a potentially novel regulator of V_2R expression and AVP sensitivity beyond the regulation of AQP2 expression. sPRR-induced V_2R expression in the CD cells is mediated by β-catenin signaling. NKCC2 expression is suppressed by S1P inhibition but is unaffected by exogenous sPRR-His, suggesting a mechanism of action of sPRR in the TAL that is distinct from that in the CD. Overall, these results offer new perspectives on the S1P/sPRR/V_2R pathway in renal control of fluid homeostasis.

Methods

Animals. Male 10- to 12-week-old C57/BL6 mice were purchased from the Jackson Laboratory, and male Sprague-Dawley (SD) rats were from Charles River Laboratories. All animals were cage-housed and maintained in a temperature-controlled room with a 12:12-hour light-dark cycle, with free access to tap water and standard rat chow for 14 days.

Conditional gene KO mouse experiments. Mice with conditional deletion of PRR in the CD (CD PRR–KO) were generated by genetic crosses between $PRR^{fl/fl}$ mice (46) and AQP2-Cre mice (47). Mice with inducible deletion of PRR (27) or S1P in the whole renal tubules (RT PRR–KO or RT S1P–KO) were generated by genetic crosses between $PRR^{fl/fl}$ or $S1P^{fl/fl}$ mice and mice containing Pax8-reverse tetracycline transactivator (Pax8-rtTA) and LC-1 transgenes. Male 10- to 12-week-old null mice and their respective littermate floxed control mice were used for all experiments. All animals were acclimatized to metabolic cages for 7 days. After collection of baseline data for 2 days, the PRR- or S1P-null mice were infused for 4 or 7 days with sPRR-His at 30 μg/kg/d via jugular vein catheterization connected to an osmotic mini-pump (Alzet model 1007D, Alza). At the end of the experiment, blood was drawn from the vena cava, and 1 kidney was cut into cortex and inner medulla; the other kidney was fixed and paraffin embedded.

Genotyping. DNA was isolated from a variety of organs and PCR was performed using the following primers: S1P, forward 5′-GAG AGC TCG AGA TGA CAG GGG ACA CAG-3′ and reverse 5′-GCC CAA TCC ACC GCT CTG TAG CGG AC-3′, which yields a 434-bp product from the $S1P^{fl/fl}$ gene and a 380-bp product from the WT allele.

Analysis of S1P gene recombination. DNA was isolated from a variety of organs and subjected to PCR analysis of the recombined S1P gene. PCR was performed for 40 cycles at 94°C for 20 seconds, 60°C for 45 seconds, and 68°C for 3 minutes and 45 seconds using the following primers: forward 5′- CAA AGG CAA GGC CTA CAG AG-3′ and reverse 5′-GAG AGC TGC AGA TGA CAGG-3′. These primers are located in introns 1 and 2 and yield an 1800-bp product from the recombined DNA product.

C57/BL6 mouse experiments. Male 10- to 12-week-old C57/BL6 mice were acclimatized to metabolic cages for 7 days. After collection of baseline data for 2 days, mice randomly received vehicle or s.c. PF infusion at 20 mg/kg/day via osmotic minipump (Alzet model 1007D, Alza) or in conjunction with i.v. sPRR-His infusion at 30 μg/kg/day via jugular vein catheterization connected to a separate osmotic minipump for 4 days. The sample collections were same as described above.

Acute AVP experiments. Urinary bladder was emptied from mice by bladder massage, and the mice were i.p. injected with AVP (720 ng/kg body weight). Over a 2-hour period in which mice had no access to food or water, urine was collected by bladder massage, and urine osmolality was measured at baseline and following AVP injection. AVP sensitivity was represented as the ratio of osmolality change.

Cell culture experiments. IMCD cells were prepared from 4-week-old SD rats as previously described (48). Briefly, the cells were grown in Transwells (catalog 29442-074, VWR) with DMEM/F-12 medium containing 10% FBS (Thermo Fisher Scientific), 0.5 μM 8-Br-cAMP (MilliporeSigma), 130 mM NaCl (Mallinckrodt Chemical), and 80 mM urea (Mallinckrodt Chemical). After 4 days of growth, the cells were serum deprived for 12 hours and pretreated with an inhibitor (1.4 μM PRO20 [in-house], 1.5 μg/ml of anti–PRR-N antibody [gift from Yumei Feng; University of Nevada, Reno, Nevada, USA], 1 μM ICG001 [catalog, Cayman], 10 μM PF [catalog HY-13447A, MedChem Express]; ref. 13), followed by 24-hour treatment with AVP (10 nM; catalog V9879, MilliporeSigma) or sPRR-His (10 nM; in-house). At the end of the experiments, the medium was collected for biochemical assays and the cells were harvested for immunoblotting.

Enzyme immunoassay. AVP and sPRR in biological fluids were determined by using the following commercially available enzyme immunoassay (EIA) kits according to the manufacturer's instructions: the kits for AVP (catalog 583951, Cayman Chemical) and sPRR (catalog JP27782, IBL).

Immunoblotting. Renal tissues were lysed and subsequently sonicated. Protein concentrations were determined by using Coomassie reagent. Protein (40 μg) for each sample was denatured in boiling water and was then separated by SDS-PAGE gels and transferred onto nitrocellulose membranes. Blots were blocked 1 hour with 5% nonfat dry milk in Tris-buffered saline (TBS), followed by incubation overnight with primary antibody. After washing with TBS, blots were incubated with goat anti–rabbit/mouse/goat horseradish peroxidase– conjugated (HRP-conjugated) secondary antibody and visualized using enhanced chemiluminescence (ECL). The blots were quantitated by using Imagepro-plus. The primary antibodies include goat anti-AQP2 (catalog sc-9882, Santa Cruz Biotechnology Inc.), rabbit anti-NKCC2 (catalog SPC401, StressMarq), rabbit anti-V_2R (catalog ab109326, Abcam), mouse anti-p62 (catalog ab40790, Abcam), and rabbit anti-LC3B (catalog ab48394, Abcam).

qPCR. Total RNA was isolated from renal tissues and reverse transcribed to cDNA. Oligonucleotides were designed using Primer3 software (available at http://bioinfo.ut.ee/primer3-0.4.0/). Primers of V_2R are: 5′-TGC TGG CGG TGA TTT TCGT-3′ (sense) and 5′-GGA AGA TGC GAACATGGCAAA-3′ (antisense); primers of NKCC2 are: 5′-GTC TCG GTG TGA TTA TCA TCGG-3′ (sense) and 5′-ATC CGT TTG TGG CGA TAG CAG-3′ (antisense); and primers for GAPDH are: 5′-GTC TTC ACT ACC ATG GAG AAGG-3′ (sense) and 5′-TCA TGG ATG ACC TTG GCC AG-3′ (antisense).

Statistics. Data is summarized as means ± SEM. All data points represent animals that were included in the statistical analyses. Sample sizes were determined on the basis of similar previous studies or pilot experiments. Statistical analysis for animal and cell culture experiments was performed by using ANOVA with the Bonferroni test for multiple comparisons or by paired or unpaired Student's *t* test for 2 comparisons. The Student's *t* tests were performed with 2-tailed *t* test. The $P < 0.05$ was considered statistically significant.

Study approval. The present studies in animals were reviewed and approved by the Animal Care and Use Committee at the University of Utah.

Author contributions

TY planned and supervised the project. TY and FW designed the research studies, analyzed the data, and wrote the manuscript. FW, CX, RL, KP, SX, XL, LZ, and CJZ contributed to conducting experiments and acquiring data. CX, NR, and DEK provided the KO animals. NR and DK commented on the manuscript.

Acknowledgments

This work was supported by National Natural Science Foundation of China grants nos. 31330037, 91439205, and 81630013; NIH grants DK104072, DK104072, HL135851, and HL139689; VA Merit Review from the Department of Veterans Affairs; and postdoctoral fellowship award 19POST34400031 from AHA. TY is a Research Career Scientist in Department of Veterans Affairs.

Address correspondence to: Tianxin Yang, University of Utah and VA Medical Center, 30 N 1900 E, Rm 4R312, Salt Lake City, Utah 84132, USA. Phone: 801.585.5570; Email: Tianxin.Yang@hsc.utah.edu.

1. Fenton RA, Knepper MA. Mouse models and the urinary concentrating mechanism in the new millennium. *Physiol Rev*. 2007;87(4):1083–1112.
2. Chabardès D, et al. Localization of mRNAs encoding Ca2+-inhibitable adenylyl cyclases along the renal tubule. Functional consequences for regulation of the cAMP content. *J Biol Chem*. 1996;271(32):19264–19271.
3. Christensen BM, Zelenina M, Aperia A, Nielsen S. Localization and regulation of PKA-phosphorylated AQP2 in response to V(2)-receptor agonist/antagonist treatment. *Am J Physiol Renal Physiol*. 2000;278(1):F29–F42.
4. Moeller HB, Fenton RA. Cell biology of vasopressin-regulated aquaporin-2 trafficking. *Pflugers Arch*. 2012;464(2):133–144.
5. Mutig K, et al. Demonstration of the functional impact of vasopressin signaling in the thick ascending limb by a targeted transgenic rat approach. *Am J Physiol Renal Physiol*. 2016;311(2):F411–F423.
6. Giménez I, Forbush B. Short-term stimulation of the renal Na-K-Cl cotransporter (NKCC2) by vasopressin involves phosphorylation and membrane translocation of the protein. *J Biol Chem*. 2003;278(29):26946–26951.
7. Nabi AH, Suzuki F. Biochemical properties of renin and prorenin binding to the (pro)renin receptor. *Hypertens Res*. 2010;33(2):91–97.
8. Nguyen G, Delarue F, Burcklé C, Bouzhir L, Giller T, Sraer JD. Pivotal role of the renin/prorenin receptor in angiotensin II production and cellular responses to renin. *J Clin Invest*. 2002;109(11):1417–1427.
9. Nguyen G. Renin, (pro)renin and receptor: an update. *Clin Sci*. 2011;120(5):169–178.
10. Ramkumar N, et al. Nephron-specific deletion of the prorenin receptor causes a urine concentration defect. *Am J Physiol Renal Physiol*. 2015;309(1):F48–F56.
11. Trepiccione F, et al. Renal Atp6ap2/(Pro)renin Receptor Is Required for Normal Vacuolar H+-ATPase Function but Not for the

Renin-Angiotensin System. *J Am Soc Nephrol*. 2016;27(11):3320–3330.
12. Trepiccione F, et al. Renal Atp6ap2/(Pro)renin Receptor Is Required for Normal Vacuolar H+-ATPase Function but Not for the Renin-Angiotensin System. *J Am Soc Nephrol*. 2016;27(11):3320–3330.
13. Wang F, et al. Antidiuretic Action of Collecting Duct (Pro)Renin Receptor Downstream of Vasopressin and PGE2 Receptor EP4. *J Am Soc Nephrol*. 2016;27(10):3022–3034.
14. Nguyen G. Renin and prorenin receptor in hypertension: what's new? *Curr Hypertens Rep*. 2011;13(1):79–85.
15. Watanabe N, et al. Soluble (pro)renin receptor and blood pressure during pregnancy: a prospective cohort study. *Hypertension*. 2012;60(5):1250–1256.
16. Lu X, et al. Soluble (pro)renin receptor via β-catenin enhances urine concentration capability as a target of liver X receptor. *Proc Natl Acad Sci USA*. 2016;113(13):E1898–E1906.
17. Cousin C, Bracquart D, Contrepas A, Corvol P, Muller L, Nguyen G. Soluble form of the (pro)renin receptor generated by intracellular cleavage by furin is secreted in plasma. *Hypertension*. 2009;53(6):1077–1082.
18. Yoshikawa A, et al. The (pro)renin receptor is cleaved by ADAM19 in the Golgi leading to its secretion into extracellular space. *Hypertens Res*. 2011;34(5):599–605.
19. Nakagawa T, et al. Site-1 protease is required for the generation of soluble (pro)renin receptor. *J Biochem*. 2017;161(4):369–379.
20. Fang H, et al. (Pro)renin receptor mediates albumin-induced cellular responses: role of site-1 protease-derived soluble (pro)renin receptor in renal epithelial cells. *Am J Physiol, Cell Physiol*. 2017;313(6):C632–C643.
21. Birnbaumer M. Vasopressin receptors. *Trends Endocrinol Metab*. 2000;11(10):406–410.
22. Machida K, et al. Downregulation of the V2 vasopressin receptor in dehydration: mechanisms and role of renal prostaglandin synthesis. *Am J Physiol Renal Physiol*. 2007;292(4):F1274–F1282.
23. Izumi Y, et al. Regulation of V2R transcription by hypertonicity and V1aR-V2R signal interaction. *Am J Physiol Renal Physiol*. 2008;295(4):F1170–F1176.
24. Memetimin H, et al. Low pH stimulates vasopressin V2 receptor promoter activity and enhances downregulation induced by V1a receptor stimulation. *Am J Physiol Renal Physiol*. 2009;297(3):F620–F628.
25. Traykova-Brauch M, et al. An efficient and versatile system for acute and chronic modulation of renal tubular function in transgenic mice. *Nat Med*. 2008;14(9):979–984.
26. Ramkumar N, Kohan DE. Role of collecting duct renin in blood pressure regulation. *Am J Physiol Regul Integr Comp Physiol*. 2013;305(2):R92–R94.
27. Ramkumar N, et al. Renal tubular epithelial cell prorenin receptor regulates blood pressure and sodium transport. *Am J Physiol Renal Physiol*. 2016;311(1):F186–F194.
28. Lu X, et al. Soluble (pro)renin receptor via β-catenin enhances urine concentration capability as a target of liver X receptor. *Proc Natl Acad Sci USA*. 2016;113(13):E1898–E1906.
29. Shan Z, et al. Involvement of the brain (pro)renin receptor in cardiovascular homeostasis. *Circ Res*. 2010;107(7):934–938.
30. Yang T. Unraveling the Physiology of (Pro)Renin Receptor in the Distal Nephron. *Hypertension*. 2017;69(4):564–574.
31. Yang T, Xu C. Physiology and Pathophysiology of the Intrarenal Renin-Angiotensin System: An Update. *J Am Soc Nephrol*. 2017;28(4):1040–1049.
32. Knoers NV, Monnens LL. Nephrogenic diabetes insipidus. *Semin Nephrol*. 1999;19(4):344–352.
33. Nielsen S, Frøkiaer J, Marples D, Kwon TH, Agre P, Knepper MA. Aquaporins in the kidney: from molecules to medicine. *Physiol Rev*. 2002;82(1):205–244.
34. Lu X, Garrelds IM, Wagner CA, Danser AH, Meima ME. (Pro)renin receptor is required for prorenin-dependent and -independent regulation of vacuolar H(+)-ATPase activity in MDCK.C11 collecting duct cells. *Am J Physiol Renal Physiol*. 2013;305(3):F417–F425.
35. Ramkumar N, Kohan DE. The nephron (pro)renin receptor: function and significance. *Am J Physiol Renal Physiol*. 2016;311(6):F1145–F1148.
36. Bachmann S, Mutig K. Regulation of renal Na-(K)-Cl cotransporters by vasopressin. *Pflugers Arch*. 2017;469(7-8):889–897.
37. Mutig K, Paliege A, Kahl T, Jöns T, Müller-Esterl W, Bachmann S. Vasopressin V2 receptor expression along rat, mouse, and human renal epithelia with focus on TAL. *Am J Physiol Renal Physiol*. 2007;293(4):F1166–F1177.
38. Rousselle A, Sihn G, Rotteveel M, Bader M. (Pro)renin receptor and V-ATPase: from Drosophila to humans. *Clin Sci*. 2014;126(8):529–536.
39. Ichihara A. (Pro)renin receptor and autophagy in podocytes. *Autophagy*. 2012;8(2):271–272.
40. Kurauchi-Mito A, et al. Significant roles of the (pro)renin receptor in integrity of vascular smooth muscle cells. *Hypertens Res*. 2014;37(9):830–835.
41. Monnerie H, et al. Reduced sterol regulatory element-binding protein (SREBP) processing through site-1 protease (S1P) inhibition alters oligodendrocyte differentiation in vitro. *J Neurochem*. 2017;140(1):53–67.
42. Brown MS, Goldstein JL. A proteolytic pathway that controls the cholesterol content of membranes, cells, and blood. *Proc Natl Acad Sci USA*. 1999;96(20):11041–11048.
43. Linser R, Salvi N, Briones R, Rovó P, de Groot BL, Wagner G. The membrane anchor of the transcriptional activator SREBP is characterized by intrinsic conformational flexibility. *Proc Natl Acad Sci USA*. 2015;112(40):12390–12395.
44. Zandberg WF, Benjannet S, Hamelin J, Pinto BM, Seidah NG. N-glycosylation controls trafficking, zymogen activation and substrate processing of proprotein convertases PC1/3 and subtilisin kexin isozyme-1. *Glycobiology*. 2011;21(10):1290–1300.
45. Ye J, et al. ER stress induces cleavage of membrane-bound ATF6 by the same proteases that process SREBPs. *Mol Cell*. 2000;6(6):1355–1364.
46. Kinouchi K, et al. The (pro)renin receptor/ATP6AP2 is essential for vacuolar H+-ATPase assembly in murine cardiomyocytes. *Circ Res*. 2010;107(1):30–34.
47. Nelson RD, et al. Expression of an AQP2 Cre recombinase transgene in kidney and male reproductive system of transgenic mice. *Am J Physiol*. 1998;275(1 Pt 1):C216–C226.
48. Wang F, et al. Prostaglandin E-prostanoid4 receptor mediates angiotensin II-induced (pro)renin receptor expression in the rat renal medulla. *Hypertension*. 2014;64(2):369–377.